Measured and Predicted Burial of Cylinders During the Indian Rocks Beach Experiment

Grant R. Bower, Michael D. Richardson, Kevin B. Briggs, Paul A. Elmore, Edward F. Braithwaite III, John Bradley, Sean Griffin, Thomas F. Wever, and Ralf Lühder

***Abstract*—Burial of instrumented mine-like cylinders as a result of wave-induced scour was measured during experiments conducted in shallow water (15–16 m) with fine-sand (133-μm) and coarse-sand (566-μm) sediments off Indian Rocks Beach (IRB), FL. Scour pits developed around the instrumented cylinders in the fine-sand site when significant waveheights exceeded 2 m, causing the cylinders to pitch, then roll into the developing scour pits, often changing heading to align parallel with the wave crest. Final cylinder burial was nearly 40 cm (about 70%–80% mine diameter) relative to the sediment–water interface, but only 20%–50% relative to surface area covered. The difference was caused by the lack of complete infilling of scour pits. Little development of scour pits and burial was noted on the coarse-sand site and the cylinders buried to only 20%–40% of the cylinder diameter below the sediment surface. Burial results, although variable, are in general agreement with the wave-induced scour model developed by Trembanis *et al.* (2007) for the fine sand, but not for the coarse sand where measured burial was much less than predicted.**

***Index Terms*—Cylinders, fluid flow, hydrodynamics, mine burial, scour, sediments.**

I. Introduction

ONE of the greatest difficulties facing mine countermeasure operations is the detection and classification of partially buried mines. On sandy sediments, bottom mines have been buried by scour from wave action or tidal currents, wave-induced liquefaction, migrating sand dunes, or changes in seafloor morphology. These burial processes are dependent on sediment type, geotechnical properties, bathymetry, meteorological conditions and history, wave action, bottom currents, and mine properties (density, size, and shape) [1], [2]. Once buried, sonar detection is difficult, especially at the long standoff distances required for mine-hunting ships. Prediction of mine burial is, therefore, a critical input to tactical decision aids that determine sonar effectiveness, rates of clearance, or whether to hunt, sweep, or avoid an area [3]. In softer, fine-grained sediment, burial at impact can be a significant contributor to overall burial [4]. The sandy sediment conditions of the field site for the experiment discussed herein precluded any significant influence of impact burial processes. As will be demonstrated, burial was primarily a result of wave-induced scour.

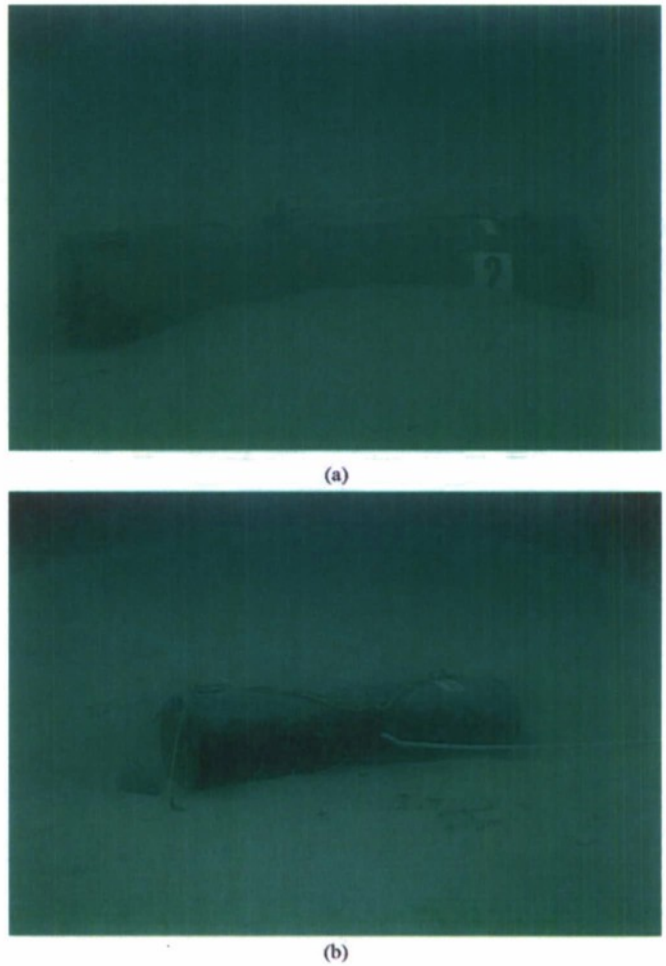

Fig. 1. Instrumented, mine-like cylinders deployed off IRB during the U.S. Office of Naval Research (ONR, Arlington, VA) burial experiments (winter–spring 2003). Underwater photographs were taken by divers just before recovery.

Omni Technologies, Inc. (New Orleans, LA) and the U.S. Naval Research Laboratory (NRL, Stennis Space Center, MS) have developed a new generation of instrumented mine-like cylindrical shapes (Fig. 1) [5], [6]. One of the key features is the 112 flush-mounted acoustic sensors intended to indicate the surface area of the cylinder covered by sediment or water (i.e., percent surface area exposed during burial) and the dimensions of the developing scour pit around the mine. The purpose of

Manuscript received May 20, 2005; revised August 10, 2006; accepted September 7, 2006. This work was supported in part by the U.S. Office of Naval Research and the U.S. Naval Research Laboratory under Base Program PE 62782N.

Guest Editor: R. H. Wilkens.

G. R. Bower, M. D. Richardson, K. B. Briggs, P. A. Elmore, and E. F. Braithwaite III are with the Marine Geosciences Division, the U.S. Naval Research Laboratory, Stennis Space Center, MS 39529 USA (gbower@nrlssc.navy.mil).

J. Bradley and S. Griffin are with the Omni Technologies, Inc., New Orleans, LA 70124 USA.

T. F. Wever and R. Lühder are with the Forschungsanstalt der Bundeswehr für Wasserschall-und Geophysik (FWG), Kiel 24148, Germany.

Digital Object Identifier 10.1109/JOE.2007.890950

0364-9059/$25.00 © 2007 IEEE

REPORT DOCUMENTATION PAGE

Form Approved
OMB No. 0704-0188

1. REPORT DATE *(DD-MM-YYYY)*	2. REPORT TYPE	3. DATES COVERED *(From - To)*
07092006	Journal Article	

4. TITLE AND SUBTITLE

Measured and Predicted Burial of Cylinders During the Indian Rocks Beach Experiment

5a. CONTRACT NUMBER

5b. GRANT NUMBER

5c. PROGRAM ELEMENT NUMBER

6. AUTHOR(S)

Grant R. Bower, Michael D. Richardson, Kevin B. Briggs, Paul A. Elmore, Edward F. Braithwaite III, John Bradley, Sean Griffin, Thomas F. Wever, and Ralf Luhder

5d. PROJECT NUMBER

5e. TASK NUMBER

5f. WORK UNIT NUMBER

7. PERFORMING ORGANIZATION NAME(S) AND ADDRESS(ES)

Naval Research Laboratory
Marine Geoacoustics Division
Stennis Space Center, MS 39529

8. PERFORMING ORGANIZATION REPORT NUMBER

NRL/JA/7430-05-10

9. SPONSORING/MONITORING AGENCY NAME(S) AND ADDRESS(ES)

Office of Naval Research
800 North Quincy Street
Arlington VA 22217-5000

10. SPONSOR/MONITOR'S ACRONYM(S)

ONR

11. SPONSOR/MONITOR'S REPORT NUMBER(S)

12. DISTRIBUTION/AVAILABILITY STATEMENT

Approved for public release; distribution is unlimited

20090522119

13. SUPPLEMENTARY NOTES

IEEE Journal of Oceanic Engineering, Vole., 32, No. 1, January 2007

14. ABSTRACT

***Abstract*—Burial of instrumented mine-like cylinders as a result of wave-induced scour was measured during experiments conducted in shallow water (15–16 m) with fine-sand (133-μm) and coarse-sand (566-μm) sediments off Indian Rocks Beach (IRB), FL. Scour pits developed around the instrumented cylinders in the fine-sand site when significant waveheights exceeded 2 m, causing the cylinders to pitch, then roll into the developing scour pits, often changing heading to align parallel with the wave crest. Final cylinder burial was nearly 40 cm (about 70%–80% mine diameter) relative to the sediment–water interface, but only 20%–50%**

15. SUBJECT TERMS

Cylinders, fluid flow, hydrodynamics, mine burial, scour, sediments

16. SECURITY CLASSIFICATION OF: a. REPORT	b. ABSTRACT	c. THIS PAGE	17. LIMITATION OF ABSTRACT	18. NUMBER OF PAGES	19a. NAME OF RESPONSIBLE PERSON
Unclassified	Unclassified	Unclassified	UU	9	Michael Richardson
					19b. TELEPHONE NUMBER *(Include area code)* 228-688-4621

TABLE I
COMPARISONS OF PHYSICAL CHARACTERISTICS

	NRL's AIMs	FWG's Instrumented Cylinders
Length:	2.032 m/(80 in)	1.499 m/(59 in)
Diameter:	0.533 m/(21 in)	0.470 m/(18.5 in)
Wt (air):	800 kg/(1764 lb)	550 kg/(1213 lb)
Wt (water):	333 kg/(735 lb)	283 kg/(624 lb)
Density:	1762 kg/m^3/(0.0636 lb/in^3)	2117 kg/m^3/(0.0765 lb/in^3)

these new instrumented mine-like cylindrical shapes is to obtain high-quality subsequent burial information (movement, scour pit development, and percent burial), as well as measure the environmental forcing (wave and currents), thereby providing a better understanding of the processes that affect burial. The four new, instrumented, mine-like cylindrical shapes are referred to as acoustic instrumented mines (AIMs). The first field exercise to use the four, new AIMs was the Indian Rocks Beach (IRB) experiment conducted in shallow water off the western coast of Florida during January–March 2003. This paper describes the experimental site (Section II), instrumented mine design features (Section III), and sediment properties and oceanographic conditions (Section IV), all of which are required inputs to predict mine burial (Section VI). Relationships between significant waveheight and cylinder movement, burial relative to the sediment water interface, and burial relative to surface area of the cylinder covered are presented in Sections IV and V. Burial recorded with other types of self-recording mine-like shapes and on multiple sediment types is also presented in Section V. A comparison of a measured to predicted burial is given in Section VI, along with diver observations that corroborate the measured burial. New insights into the scour burial process are included in Section VII.

II. DESCRIPTION—IRB EXPERIMENT

The NRL field experiment in winter 2003 involved deployment, recovery, and diver inspection of ten instrumented mine-like shapes at three different sites and collection of sediment samples for laboratory analysis. In addition to the four AIMs, the other instrumented mine-like shapes used for this experiment included six Forschungsanstalt der Bundeswehr für Wasserschall und Geophysik (FWG, Kiel, Germany) mine-like cylinder shapes which use optic sensors to measure the surface area of each cylindrical shape covered by sediment [7]. All of the AIMs and two FWG cylinders were deployed at the same general location on fine-sand sediment at about 15-m water depth. Two FWG mines were also deployed at each of two other sites selected nearby, one on coarse-sand sediment and the other on a slightly deeper (16-m water depth) fine-sand sediment site. Additional details of the experiment are available in [8].

III. DESCRIPTION OF THE AIMS

A. Mechanical Overview

The instrumented, bronze, and mine-like shapes are blunt-ended cylinders with a 0.53-m diameter and a 2.03-m length. They have a fully loaded mass of approximately 900 kg and an average density of 1980 kg/m^3. Table I compares the physical characteristics of the AIMs to the FWG cylinders. The mine shapes incorporate flush-mounted transducers to maintain a smooth outer surface to minimize unwanted turbulence from protrusions. Nearly all of the electronics are housed in a second pressure vessel within the main shape to provide secondary protection in the event of a leak. A more detailed physical and operational description of the AIMs is reported by Bradley *et al.* [6] and only the sensors used for this paper are described as follows.

B. Burial Sensors

There is a total of 112 acoustic burial transducers installed on the surface of each mine—six sensors in each end cap and ten rings of ten sensors evenly distributed over the cylinder surface. The acoustic burial transducers are designed to provide data to determine the burial state (covered or not covered) of each sensor. Data from the acoustic burial sensors can be analyzed to characterize the physical characteristics and dynamic changes of the scour pit surrounding the mine-like shapes.

C. Orientation Sensors

The orientation sensors consist of a commercial (off-the-shelf), three-axes flux gate compass and three-axes accelerometer for roll and pitch. Heading accuracy is approximately $\pm 2.0°$ and roll/pitch accuracy is approximately $\pm 0.5°$.

D. Pressure Sensors

Six pressure sensors monitor changes in bottom water pressure fluctuations [0–700 kPa (0–100 in/lb^2) sampled at 10 Hz] and provide input to calculate mean water depth and surface waveheight and period. Comparison of the water depth changes (as measured by the pressure sensors) to other nearby tidal measurements is used to estimate burial of the cylinders relative to the water–sediment interface.

IV. ENVIRONMENTAL MEASUREMENTS

A. Surface Sediment Description

The experiment site was located 20 km west of IRB, in 15–16-m water depth in an area of mostly fine-sand sediment punctuated with coarse-sand rippled scour depressions (RSDs) [9], [10]. Sediment samples were obtained with diver-collected cores and grain size and porosity were measured at 2-cm intervals. The grain-size distributions were determined by dry-sieving the sand fractions at quarter–phi intervals, by pipette for assaying the silt and clay fractions, and by employing the graphic statistical techniques described by Folk and Ward [11]. Porosity and density values were determined from accurate measurements of water loss during oven-drying from each 2-cm interval

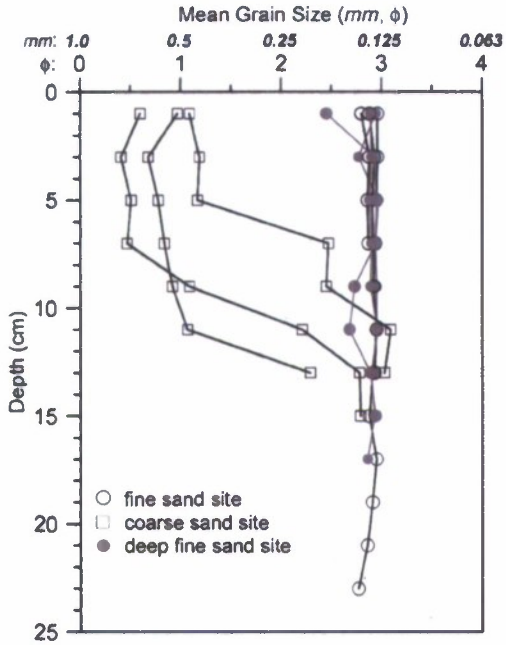

Fig. 2. Vertical profiles of sediment mean grain size as a function of depth in the sediment for the three sites within the experiment area.

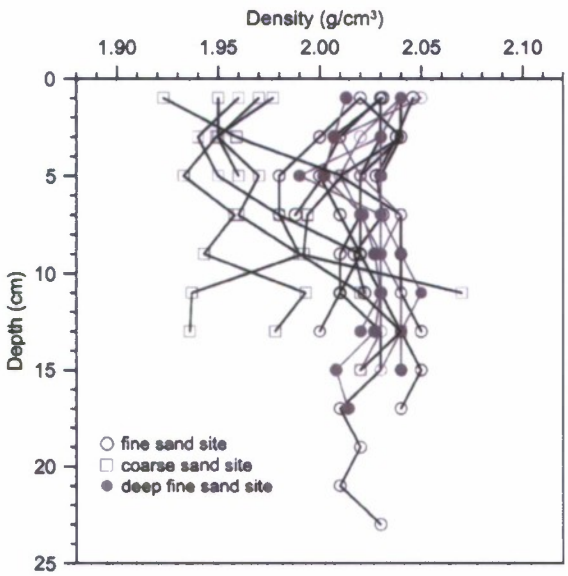

Fig. 3. Vertical profiles of sediment bulk density as a function of depth in the sediment for the three sites within the experiment area.

and grain density from the dried sample intervals. The fine-sand sediment was well sorted to very well sorted, coarse-skewed, leptokurtic, quartz sand with a graphic mean and median (D_{50}) grain size of 2.89ϕ (135μm). The sediment within the RSD was poorly sorted, strongly fine-skewed, very leptokurtic, coarse quartz sand with mollusk shell fragments and had a graphic mean grain size of 0.84ϕ (559 μm) and a D_{50} of 0.53ϕ (693 μm). The coarse sand was 10–15 cm thick and overlaid fine sand that was similar to the sand making up the shelf sediments outside the RSD. Three sites were chosen to deploy the mines: one on fine sand in 15-m water depth, another one in an RSD with coarse sand also in 15-m water depth, and a third one on fine sand in

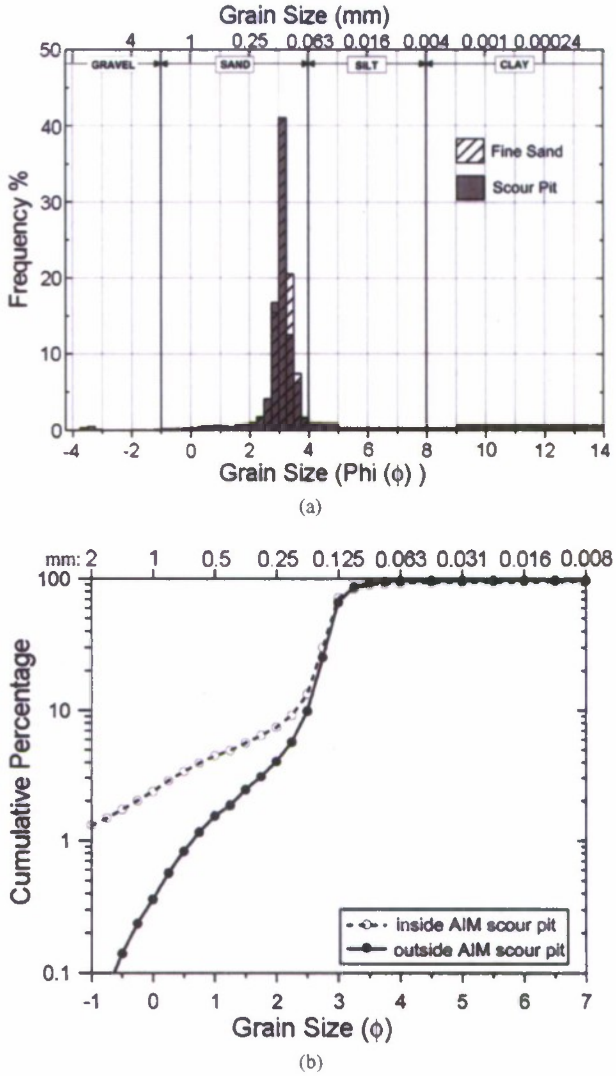

Fig. 4. (a) Comparison of average grain-size distribution histograms from the fine-sand site and from sediments collected from the scour pits surrounding those mines. (b) Cumulative grain-size distribution curves for the data in (a).

16-m water depth. Values of sediment bulk density and mean grain size for the three sites were measured at 2-cm intervals from diver cores collected in January and March 2003 (Figs. 2 and 3). The thin veneer of coarse sediment overlying finer sediment can be seen in the sediment depth profiles measured from the RSD. The coarser sand in the top 10 cm in the RSD has a slightly lower average bulk density [1958 ($\pm$23.3) kg/m^3] than the finer sand outside the RSD [2013 ($\pm$023.8) kg/m^3] and the fine-sand sediment found below the coarse-sand sediment [1997 ($\pm$43.2) kg/m^3]. In either case, the bulk density of the sediment and the instrumented mines were nearly identical.

B. Sediments in Scour Pits

Just before recovery of AIMS, sediments were collected using diver cores from the scour pits surrounding the four AIMs and two of the six FWG self-recording cylindrical shapes. Diver sediment cores (four) were also collected in the general vicinity of the cylindrical shapes. Sediments from the scour pits associated with the AIMs (Fig. 4) contained gray

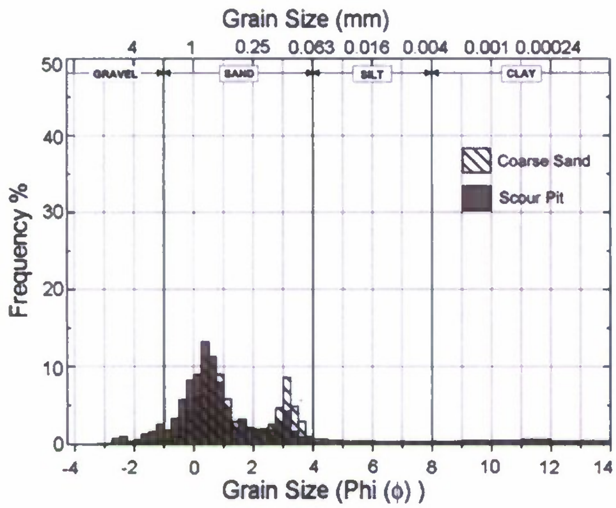

(a)

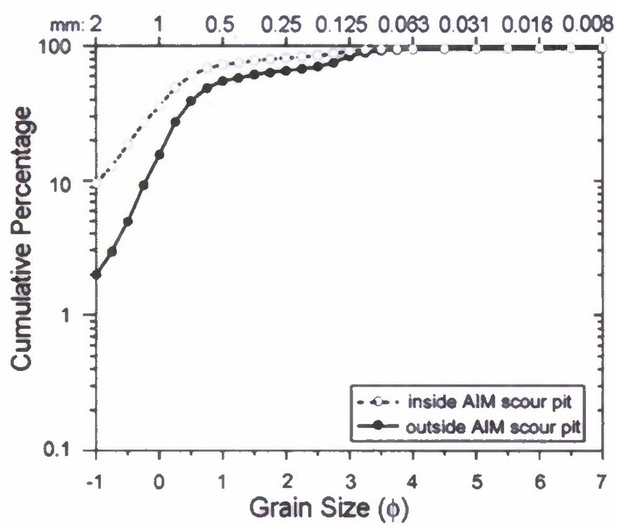

(b)

Fig. 5. (a) Comparison of average grain-size distribution histograms from the coarse-sand site and from sediments collected from the scour pits surrounding those cylinders. (b) Cumulative grain-size distribution curves for the data in (a).

mud deposits as well as shell lag deposits, with an average mean grain size of 2.90ϕ (134 μm). It appears that sediments in the scour pits experienced winnowing out of the fine sand (3.5–4.0ϕ), an increase in coarser shell hash (-3 to -4ϕ), and an increase in the silt and clay fraction. In the scour pits associated with the FWG cylindrical shapes in the coarse-sand site, sediments were more characteristic of the top 10–12 cm of coarse sand, rather than the finer sand beneath the coarse-sand veneer. However, there was evidence of winnowing of coarse- and medium-sand-sized particles, and an increase in the proportion of gravel-sized particles (Fig. 5). The values of the mean grain size of these scour fill sediments was 0.69ϕ. (620 μm) compared to 0.84ϕ (559 μm) for the top 10 cm of sediment from the surrounding area.

C. *Oceanographic Measurements and Mine Movement*

Fig. 6 displays the heading, pitch and roll angle, and significant waveheight recorded by the four AIMs. AIM1 experienced only slight changes in the heading (less than 5° during the entire deployment) that corresponded to periodic increases in the significant waveheight. Changes in heading were accompanied with rapid changes in pitch and a significant roll (up to 30°). The data suggest significant waveheights greater than 2 m cause scour around the cylindrical shapes. After a significant amount of scour occurs, the cylinder begins to pitch, and then rolls into the scour pit, changing heading to align parallel with the waves. AIM2 made a total heading change of about 9° during the entire deployment with the changes occurring within the first 15 days and corresponding to the significant waveheight events exceeding 2 m. Similar changes in pitch and roll accompanied heading changes but were restricted to storms on day dates 18 (January 18) and 24–25 (January 24–25). AIM3's changes in heading closely mimicked those of AIM1 but had roughly double the amplitude. The total roll for the deployed period was about 30° (although in the opposite direction as AIM1). AIM4's heading closely mimicked AIM2 heading changes (and amplitude) and corresponded with the increases in significant waveheight; however, AIM4 rolled in the opposite direction compared to AIM3. After the initial two significant scour events, additional scour around the AIM3 and AIM4 was not sufficient to cause a detectable change in orientation.

Fig. 7 displays the temperature, tide, wave period, and significant waveheight measured by AIM1 which is nearly identical for each of the four AIMs. The wave direction, as measured by a downward looking Sontek pulse-coherent acoustic Doppler profiler (PC-ADP) mounted on the University of South Florida's (Tampa, FL) Quadpod, was generally easterly or onshore (Fig. 8). The Quadpod was deployed within a few meters of AIM3. Although all mine-like shapes were deployed on sand sediment (fine or coarse) and experienced similar forcing from waves and currents, significant differences in behaviors resulting in burial were noted.

V. Mine Burial Results

A. *AIMS Burial (Relative to the Sediment–Water Interface)*

An estimate of the AIMs' burial relative to water-sediment interface was calculated by subtracting the National Oceanic and Atmospheric Administration (NOAA) recorded tide data from relative tide data derived from the mean pressure recorded in each AIM (mean of all six pressure sensors for each mine). Fig. 9 is the graphical representation of these data after lowpass filtering (3-dB down point was 0.25 Hz) of both pressure series and tidal data to smooth the burial predictions.

Burial of all the AIMs, relative to the water-sediment interface, changed very little (maximum burial about 10 cm) until day date 18 (January 18) when the significant waveheights increased substantially (2.5–3 m) and all cylinders exhibited pitch and roll motion and changed heading (Fig. 4). Burial increased to about 25–40 cm (which is roughly 50%–75% of the AIMs diameter). Note that the experiments began on day date 8 (January 8); therefore, day date 18 is approximately ten days after the experiments began. A second storm with 2.5–3.0 m significant waveheights on day dates 24–25 (January 24–25) is correlated with additional cylinder movement and burial to 45–50-cm depth. After day date 25 (January 25), only AIMs 1 and 3 ex-

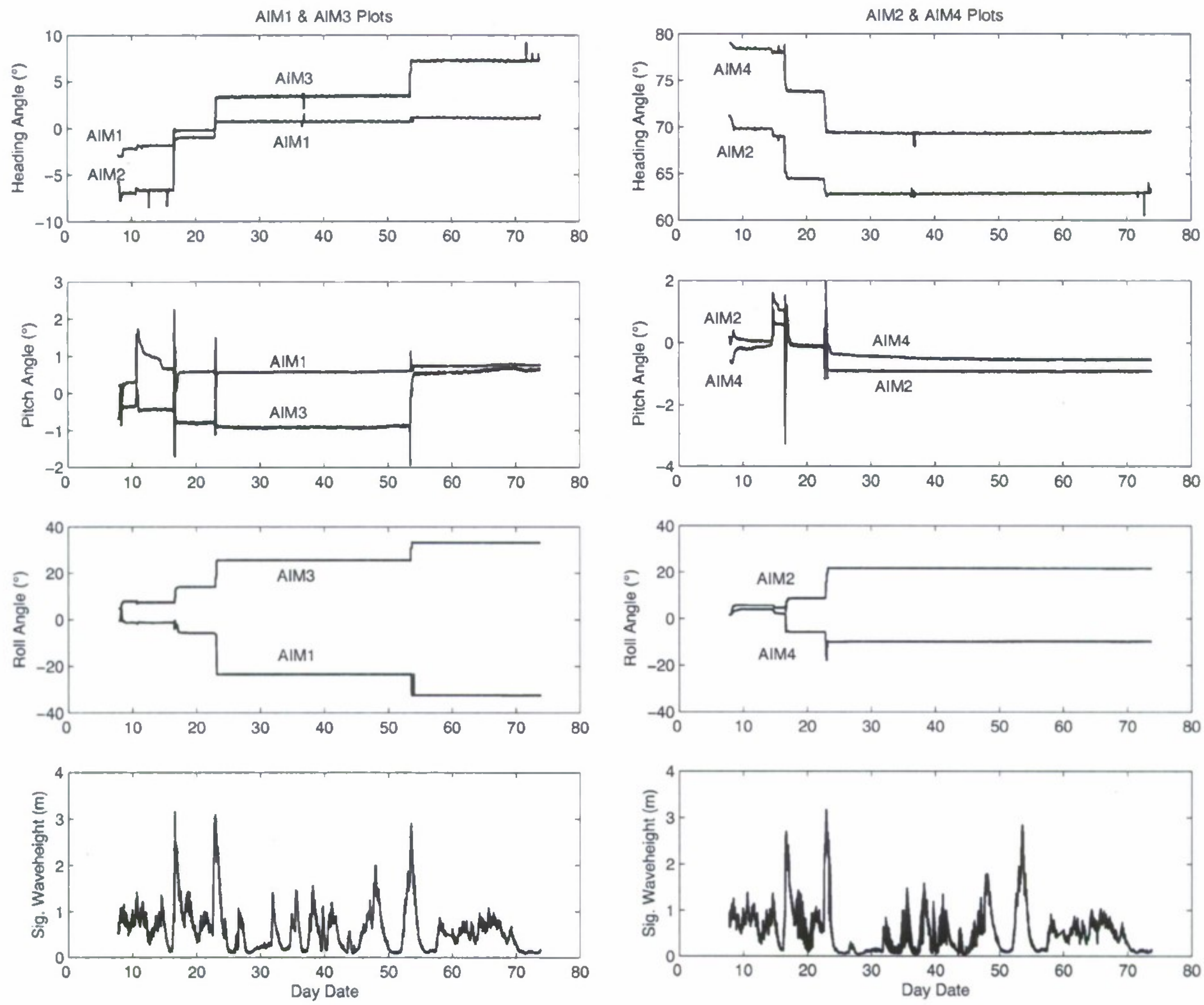

Fig. 6. Changes in orientation compared to significant waveheight for the four AIMs during the IRB deployment. Day date 1 begins at 00:00:00Z January 1, 2004.

hibited any motion, and this was correlated with a storm on day date 55 (February 24).

B. AIMs Burial Measured as Percent Surface Area/Sensors Covered

Simple examination of the differences in acoustic return intensity measured by the AIMs acoustic burial sensors were insufficient to unambiguously distinguish between water and sediment in contact with the sensor face. A comparison between transducers known to have been in constant contact with the seafloor [Fig. 10(a)] to transducers known to have never been in contact with the sediment [Fig. 10(b)] demonstrates both the problem and part of the solution. The acoustic returns for both acoustic sensors appear to be essentially the same for the first 45 days. After day date 53 (February, 22), transducer # 31 exhibits a fairly robust return from a distance of about 45 cm defining the wall of the scour pit. This change corresponds to a cumulative roll of AIM1 of about 30° changing the location of sensor # 31 from 36° to 66° from the center line at the top of the mine. During the course of the experiment, the sediment surface was evident in nearly 80% of the rings, allowing unambiguous determination of burial state for these rings. In other cases, as illustrated in Fig. 10(c), scattering from particles within the water column was evident indicating transducer faces that were exposed to the water column. The remaining ambiguities were resolved using diver observations during and just before recovery and video collected from a remotely operated vehicle (ROV) deployed by D. Mallision from the University of South Florida during the deployments (February 6). Diver and video observations of the state of burial of specific sensors and overall estimates of percent surface area covered from video and photographs showed excellent agreement with burial determined from the cylinder orientation and acoustic sensors demonstrating the validity of the approach. Fig. 11 depicting the percent of acoustic burial sensors covered was, therefore, developed from the acoustic transducer sensor data, as well as the orientation data, numerous photographs, and videos taken during the experiment, as well as diver observations.

All four of the AIMs were located within a 65-m perimeter and on a fine-sand sediment. Initially, between 20%–30% of the acoustic transducers were covered with sand, corresponding to a 5–10-cm burial of the cylinders below the sediment surface. The greatest changes in percent surface area buried occurred during the storms on day dates 18 (January 18), 24–25 (January 24–25),

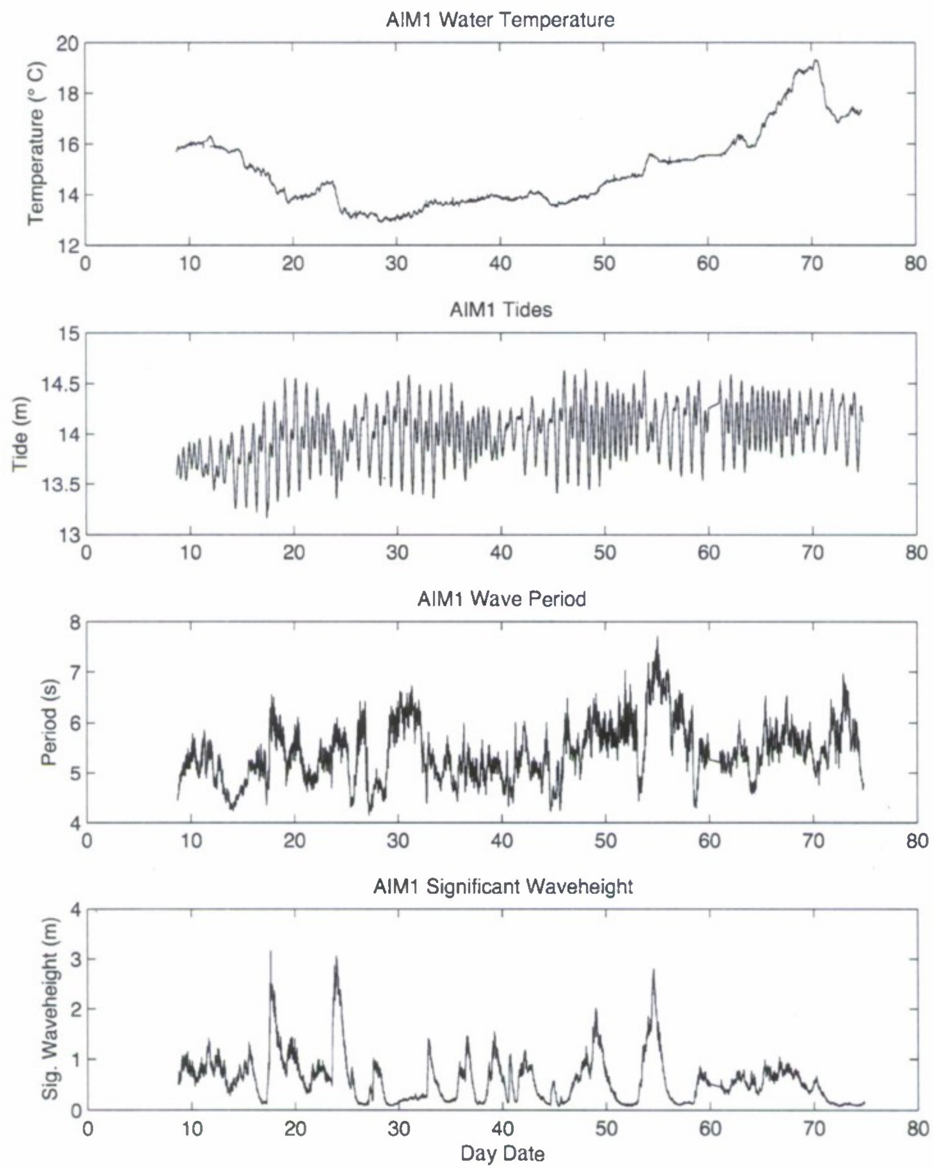

Fig. 7. Environmental conditions measured during the IRB experiments using AIM1. The results from the other AIMs were nearly identical to AIM1.

and 54–55 (February 23–24) correlating with mine movement depicted in Fig. 4. AIMs 1 and 3, which were deployed in a north–south orientation, followed similar pattern of burial. The percentages of sensors covered with sediment increased slightly with the first significant storm event on day date 18 (January 18); then, on day dates 24–25 (January 24–25), the greatest burial increase occurred corresponding to the second significant storm event. The percentages of sensors covered remained relatively stable until day date 55 (February 24) when a third storm apparently scoured sand from around AIMs, exposing roughly the same surface area as the initial burial state. The burial state remained at this level for the remainder of the experiment.

AIMs 2 and 4, which were deployed in an east–west orientation, also followed a similar pattern of burial. Surface area burial increased very slightly with the first significant storm event on day date 18; then, on day dates 24–25, a substantial increase in surface burial occurred with the second significant storm event. AIMs 2 and 4 remained relatively stable until the significant storm event of day date 55 when these AIMs buried to approximately 50%, the most burial achieved by any of the AIMs. The burial state remained at this level for the remainder of the experiment. The most significant difference in burial (percent surface area covered) among the AIMs occurred during the third storm event (day date 55) when the north–south-oriented AIMs (1 and 3) were reexposed by scour whereas the east–west-oriented AIMs (2 and 4) were buried.

There are also six acoustic sensors on each end cap, 12 end-cap sensors for each AIM. At no time were more than three end-cap sensors (out of the 12 possible sensors) covered for any AIM. The data indicate that the few sensors on the end caps that did become covered only remained so for a few days at a time. It is probable that increased scour from vortex shedding at the end of each cylinder contributes to the lack of coverage of the acoustic sensors by sand, as this has been documented

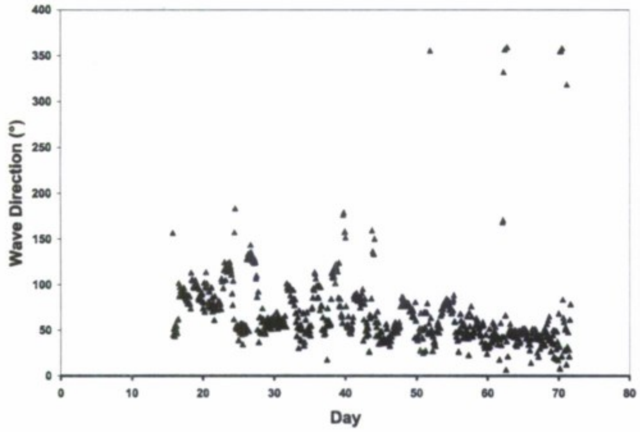

Fig. 8. Dominant wave direction measured using an ADCP deployed by Peter Howd (USF) at the fine-sand site during the IRB experiments.

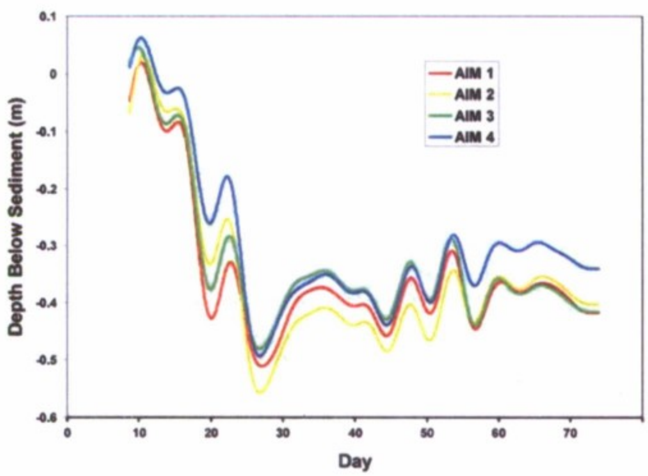

Fig. 9. Estimated burial of AIMs relative to sediment–water interface determined from differences in pressure series measured using the AIMs and mean tides.

before [12]. The phenomenon of increased scour at the ends of cylindrical shapes is corroborated by both our diver and video observations, and suggests that the end caps may be ignored in terms of a contribution to surface area burial [13].

C. Comparison of Burial of AIMs to the FWG-Instrumented Mine Shapes

I. Stender of FWG first developed self-recording cylindrical mine-like shapes that use optical methods to record the cylinder burial state [7]. Burial is measured by three rings of 24 paired optical sensors externally mounted at even intervals around the cylinders. Transmitting optical sensors are light-emitting diodes (LEDs) and receiving optical sensors are phototransistors. Burial is detected by blockage of the light beam between these sensors and it is measured as a function of surface area covered. The FWG-instrumented cylinders do not include pressure sensors to calculate burial relative to the water-sediment interface. However, diver observations at the time of recovery indicated that the FWG-instrumented cylinders on the fine-sand substrate buried 80%–90% relative to the sediment surface and 20%–40% below the sediment surface on the coarse-sand substrate.

Burial recorded on all four of the FWG instrumented cylinders (Fig. 12) deployed on the fine-sand substrate (FWG 5, 6, 9, and 10) exhibited similar trends to the AIMs with burial increasing during storm events. The percent burial rarely exceeded 40% of the sensors covered which is the same as experienced by the AIMs. These data coupled with diver and video observations suggests that, although the FWG instrumented cylinders buried to almost their full diameter (47 cm) relative to the water-sediment interface, the scour pits were never completely filled and the surface area of the cylinders remained exposed. The FWG-instrumented cylinders deployed on coarse sediments had 49% (FWG 7) and 22% (FWG 8) of the surface area covered at the end of the experiment. These differences reflect the different orientation of the cylinders to the ripple field (FWG 7 parallel and FWG 8 perpendicular to the strike of the ripples) and the fact that FWG 7 was located on a ripple crest. It is interesting to note that the orientation of the FWG cylinders at deployment did not result in the same temporal pattern of percent burial as followed by the AIMs. Changes in mine behavior, especially roll and surface area buried, exhibit considerable variability even for mines located on the same substrate and exposed to the same forcing conditions (bottom currents and significant waveheights).

VI. Mine Burial Predictions

Predictions of burial relative to the ambient level of the seabed (Fig. 13) were made using the implementation in [13] of the HR Wallingford, Wallingford, United Kingdom, scour model [14], [15]. The predictions of scour are based on the assumption of no scour-pit infilling and are plotted against experimental data (Fig. 9). The measured median grain sizes are 135 and 693 μm for fine and coarse sediments, respectively (these sizes differ from those used in [13]). Time-series input (Fig. 7) to the model was constructed from an average of the significant waveheight and peak period data obtained from sensors within the AIMs cylinders (validation given in [5]). These data were interpolated using the piecewise cubic Hermite polynomial interpolation [16] algorithm in MATLAB [17] before calculating a mean time series to get data series of equal length and equivalent starting and ending times. Burial data from the four AIMs cylinders (Fig. 9) were similarly interpolated and averaged to obtain the single mean burial time series.

Estimates of the uncertainty in the measured burial data (Fig. 14) were made from the standard deviation of the time-series data. Uncertainties in burial predictions were estimated from the differences in predictions using the upper and lower bounds for the orbital velocities as defined later and the 25th (117 μm for fine site and 150 μm for coarse site) and 75th (149 μm for fine site and 871 μm for coarse site) percentiles of the grain-size distributions [c.f. Figs. 4(b) and 5(b)]. Orbital velocity is computed from the linear wave approximation [14]

$$U_b(H_s, T_p) = \pi H_s/\sqrt{2}T_p \sinh(k_p z) \quad (1)$$

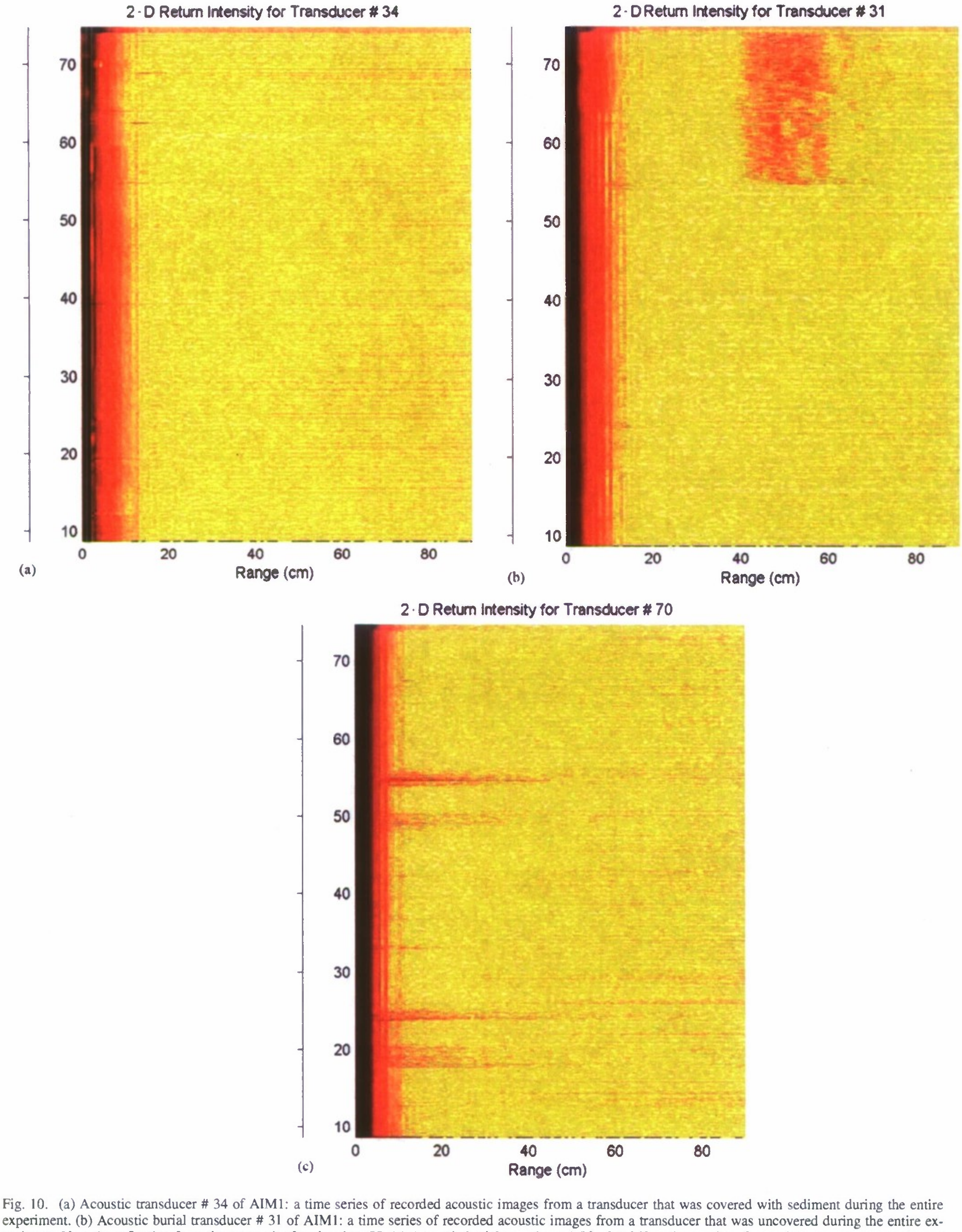

Fig. 10. (a) Acoustic transducer # 34 of AIM1: a time series of recorded acoustic images from a transducer that was covered with sediment during the entire experiment. (b) Acoustic burial transducer # 31 of AIM1: a time series of recorded acoustic images from a transducer that was uncovered during the entire experiment. Note the reflection from the scour pit after day date 55. (c) Acoustic burial transducer # 70 of AIM3: a time series of recorded acoustic images from a transducer that was uncovered during the entire experiment. Note the reflections from sand suspended in the water column that correspond to storm periods with higher significant waveheights (see Fig. 7).

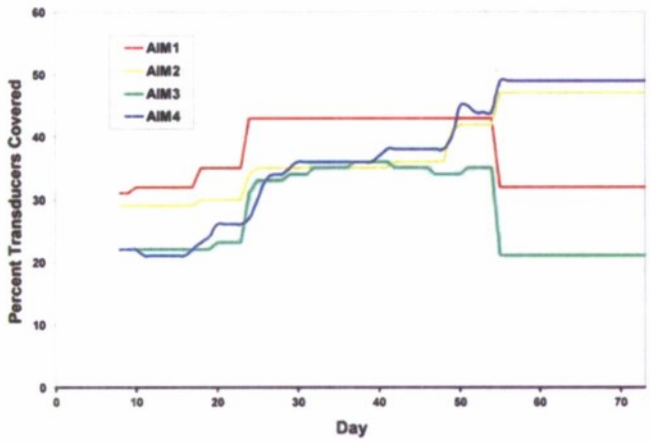

Fig. 11. Daily summary of percent transducers covered with sediments (percent burial) for the AIMs.

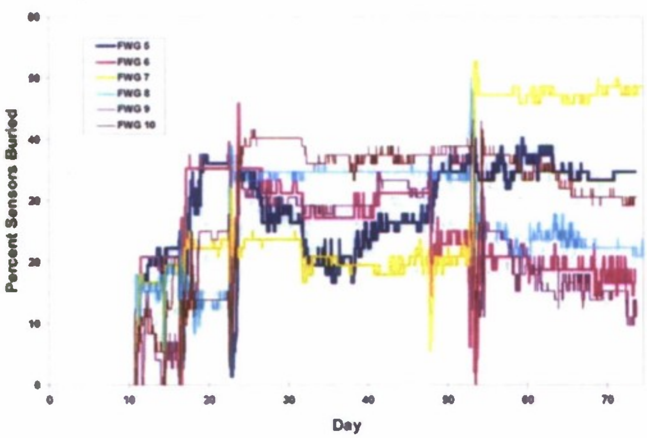

Fig. 12. Summary of percent sensor covered for the six FWG instrumented cylinders. FWG cylinders 7 and 8 were deployed in coarse-sand sediment and the remaining cylinders were deployed in fine-sand sediments.

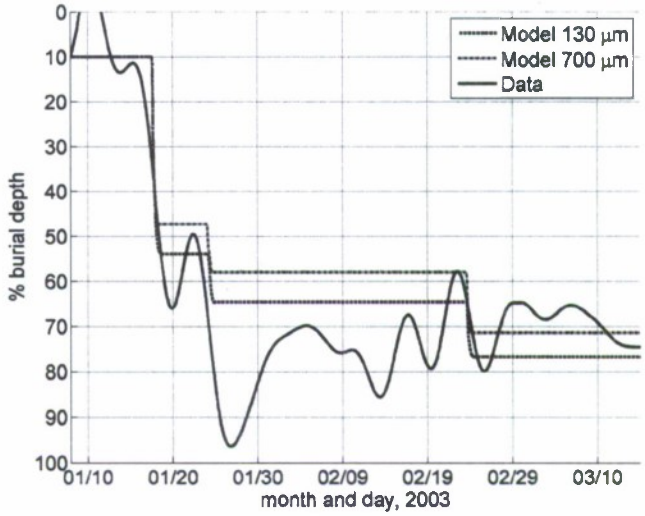

Fig. 13. Modeling predictions of burial versus mean of experimental data from Fig. 7. The two model runs are for the median grain sizes listed in the legend and at a depth of 15 m. The third line is the time-series data for the average burial depth for the four AIMs.

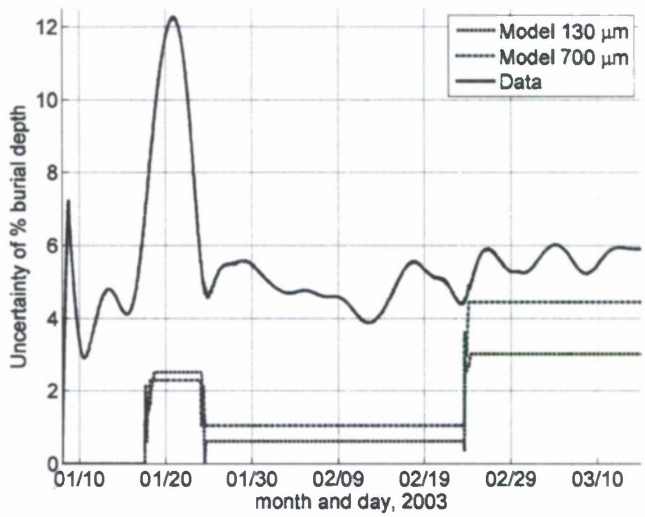

Fig. 14. Standard deviation of experimental data in Fig. 7 and total difference in model predictions obtained from the upper and lower bounds of the computed orbital velocity and the 25th and 75th quartiles of the grain size. These quartiles are 117 and 149 μm for the 135-μm site and 150 and 841 μm for the 693-μm site, respectively.

where H_s is a significant waveheight, T_p is a peak period, z is depth, and k_p is a peak wave number (calculated using T_p and z in [13, eq. (52a) and (52b)]). Thus, the upper and lower bounds for the orbital velocity are, respectively, $U_{b+} = U_b(H_s + \sigma_{H_s}, T_p - \sigma_{Tp})$ and $U_{b-} = U_b(H_s - \sigma_{H_s}, T_p + \sigma_{Tp})$.

For fine sediments, the modeled burial depth seems to qualitatively agree with measured burial depth within the uncertainties of the measured and predicted burial until the end of January. Underprediction occurs throughout February by approximately 10%, which is slightly larger than the total uncertainty (6%). There also is an apparent long-term decrease in burial depth, which is unaccounted for in the scour model. These predictions also agree qualitatively with similar burial predictions in [13] that were generated by driving the scour model with transformed WaveWatch-III [18] wave data.

For coarse sediments, there is considerable disagreement between prediction (71% burial) and measurements (20%–40% burial depth; c.f. Section V-C). In fact, diver observations [8] indicate that no scour pits were apparent surrounding any of the cylinders on coarse sediment. A couple of burial mechanisms unaccounted for in the burial model, along with the orientation of the mines relative to the ripple field, may help explain these observations. First, as discussed in [13], the presence of the sand ripple field appears to inhibit burial once the height of the mine above the seafloor is approximately 1.3 times the height (peak-to-trough) of the sand ripples. The observed sand ripple height was 15–20 cm, making the maximum predicted burial 45%–59%, which is in better agreement with the burial of the FWG cylinder that was positioned parallel to the strike of the sand ripples [Fig. 15(a)]. The FWG cylinder that was deployed and remained perpendicular to the strike of the sand ripple field [Fig. 15(b)] may have had even less burial because the mine straddled a trough in the sand ripple field

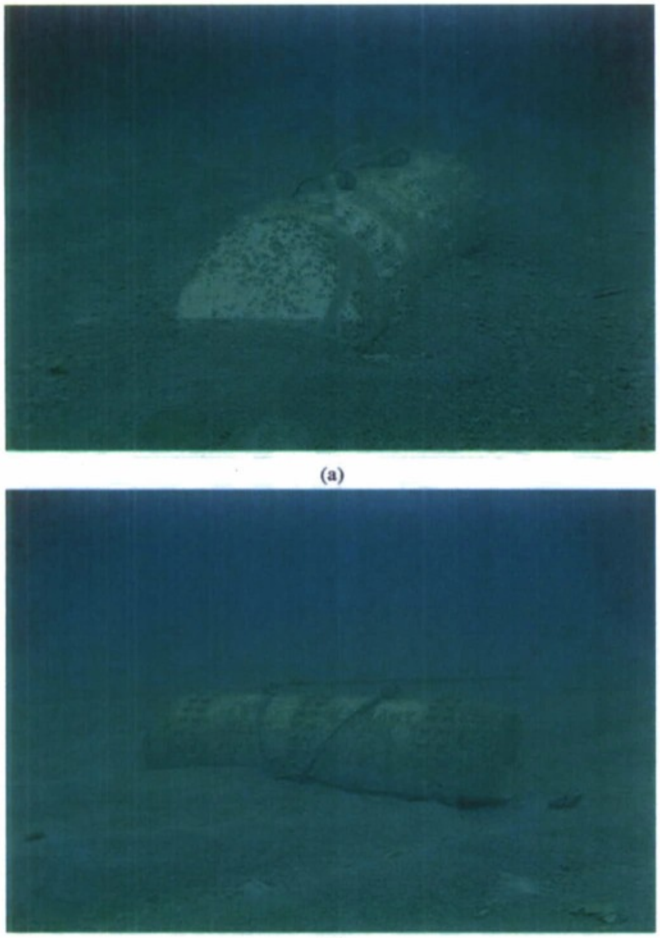

(a)

(b)

Fig. 15. FWG cylinder burial deployed on the coarse rippled seafloor. (a) FWG 7 which was deployed parallel to the strike of the ripple field had 49% of the sensors covered at the end of the experiment yet was only buried to about 30%–40% below the sediment surface. (b) FWG 8 which was deployed perpendicular to the strike of the ripple field had 22% of the sensors covered at the end of the experiment and was buried 20%–30% below the sediment surface.

(the sand ripple wavelength was 1.0–1.2 m). Second, as discussed in Sections IV-A and IV-B, the coarse-sand distribution included gravel-sized particulates that remained after sand was winnowed from underneath the cylinder (Fig. 5). This increase in percent gravel may have had an armoring effect on the bed, inhibiting scour. The model does not account for this effect since a homogenous grain size is assumed. This winnowing effect also is seen for the fine-sand site (Fig. 4), but the percentage of gravel was significantly smaller than the coarse grain site.

VII. Conclusion

There are two, somewhat independent measurements of burial that were determined by the AIMs: burial relative to the sediment–water interface and surface area covered. Burial relative to water–sediment interface was calculated using the difference between pressure series measured at the cylinder surface and the mean tidal conditions. Burial by surface area covered was measured using acoustic sensors flush mounted to the cylinder surface. The AIMs deployed on fine-sand substrate sank nearly 40 cm below the sediment–water interface by the end of the experiments, whereas, burial measured as percent surface area covered was 21%–49% by the end of the experiment. The lower percentage surface area burial was caused by incomplete infilling of the scour pits. Burial states were confirmed by visual observations made by divers and a video camera attached to an ROV. Orientation sensors demonstrated burial behavior during storms. In response to scour pit development, the cylinders began to pitch, then roll into the developing scour pit, often reorienting with the axis parallel to wave propagation. Storms with greater significant waveheights further buried the cylinders until the exposed surface area of the cylinders was too insignificant to create sufficient turbulence for further scour pit development. Large scour pits did not appear to develop around FWG instrumented cylinders deployed on coarse-sand sediment and the cylinders only buried perhaps 10–20 cm below the seafloor. Burial as measured by surface area covered of the FWG mines on the coarse-sand sediment was highly variable and primary related to orientation relative to the sand ripple field. Predicted burial using the wave-induced scour model was in general agreement with observations for fine sediments but was overpredicted for the coarse-sand sediment site. These observations suggest that some burial physics remains unaccounted for in the model.

Acknowledgment

The authors would like to thank the captain and crew of the R/V Suncoaster, who exhibited excellent seamanship for both the deployment and recovery of all the equipment; the divers R. Ray, R. Fisher, R. Brown, and C. Vaughan for positioning the equipment on the seafloor, making detailed observations of the mines and sediments, and recovering the cylinders; C. Kennedy for preparing the instrumentation for deployment and providing logistical support during the experiments; D. Naar and B. Donahue of the University of South Florida (USF) for providing logistics support, precision navigation of the ship, and invaluable support aboard the ship during the deployment and recovery; and P. Howd and D. Mallision (USF) for providing data of bottom currents from tetrapods and video images of the mines using an ROV, respectively.

References

[1] M. D. Richardson and P. Traykovski, "Real-time observations of mine burial at the Martha's Vineyard Coastal Observatory," in *Proc. 5th Int. Symp. Technol. Mine Problems*, Monterey, CA, 2002, CD-ROM.

[2] M. D. Richardson, P. J. Valent, K. B. Briggs, J. Bradley, and S. Griffin, "NRL mine burial experiments," in *Proc. 2nd Aust.-Amer. Joint Conf. Technol. Mine Countermeas.*, Sydney, Australia, 2001, CD-ROM.

[3] S. Rennie, A. Brandt, and N. Plant, "A probabilistic expert system approach for sea mine burial prediction," *IEEE J. Ocean. Eng.*, vol. 32, no. 1, pp. 260–272, Jan. 2007.

[4] C. P. Aubeny and H. Shi, "Effect of rate-dependent soil strength on cylinders penetrating into soft clay," *IEEE J. Ocean. Eng.*, vol. 32, no. 1, pp. 49–56, Jan. 2007.

[5] S. Griffin, J. Bradley, and M. D. Richardson, "Improved subsequent burial instrumented mines," *Sea Technol.*, vol. 44, no. 11, pp. 40–44, 2003.

[6] J. Bradley, S. Griffin, M. Thiele, M. D. Richardson, and P. D. Thorne, "An acoustic instrumented mine for studying subsequent burial," *IEEE J. Ocean. Eng.*, vol. 32, no. 1, pp. 64–77, Jan. 2007.

[7] T. Wever, R. Lühder, and I. Stender, "Burial recording mine—30 years of seafloor-mine-interaction research," *Sea Technol.*, vol. 45, pp. 15–19, 2004.
[8] G. R. Bower *et al.*, "Indian Rocks Beach experiment January–March 2003," NRL, Stennis Space Center, MS, Memorandum Rep., 2004.
[9] D. A. Cacchione, D. E. Drake, W. D. Grant, and G. B. Tate, "Rippled scour depressions on the inner continental shelf off central California," *J. Sediment. Petrol.*, vol. 54, no. 4, pp. 1280–1291, 1984.
[10] M. O. Green, C. E. Vincent, and A. C. Trembanis, "Suspension of coarse and fine-sand on a wave-dominated shoreface, with implications for the development of rippled scour depressions," *Continental Shelf Res.*, vol. 24, no. 3, pp. 317–335, 2004.
[11] R. L. Folk and W. C. Ward, "Brazos river bar, a study in the significance of grain size parameters," *J. Sediment. Petrol.*, vol. 27, pp. 3–26, 1957.
[12] J. Fredsøe, "Turbulent boundary in wave-current motion," *J. Hydraul. Eng. ASCE*, vol. 110, no. 8, pp. 1103–1120, 1984.
[13] A. C. Trembanis, C. T. Friedrichs, M. D. Richardson, P. A. Traykovski, P. A. Howd, P. A. Elmore, and T. F. Weaver, "Predicting mine scour burial at Indian Rocks Beach, FL and Martha's Vineyard, MA," *IEEE J. Ocean. Eng.*, vol. 32, no. 1, pp. 167–183, Jan. 2007.
[14] R. Soulsby, *Dynamics of Marine Sands: A Manual for Practical Applications*. London, U.K.: Thomas Telford, 1997.
[15] R. J. S. Whitehouse, *Scour at Marine Structures: A Manual for Practical Applications*. London, U.K.: Thomas Telford, 1998.
[16] F. N. Fritsch and R. E. Carlson, "Monotone piecewise cubic interpolation," *SIAM J. Numer. Anal.*, vol. 17, pp. 238–246, 1980.
[17] *"MATLAB,"* ver. 7.0.4, The MathWorks, Inc., 2005.
[18] H. L. Tolman, B. Balasubramaniyan, L. D. Burroughs, D. V. Chalikov, Y. Y. Chao, H. S. Chen, and V. M. Gerald, "Development and implementation of wind-generated ocean surface wave models and NCEP," *Weather and Forecasting*, vol. 17, pp. 311–333, 2002.

Grant R. Bower received the B.S. degree in electrical engineering from the Pennsylvania State University, University Park, in 1979 and the M.S. degree in management from the Florida Institute of Technology, Melbourne, in 1991.

He began working at the U.S. Naval Oceanographic Office, Stennis Space Center, MS, in 1980, where he was in the development of oceanographic instrumentation. He has participated in many at-sea field experiments. In 1990, he began working at the U.S. Naval Research Laboratory, Stennis Space Center, MS, where he has been involved with mine burial related research.

Michael D. Richardson received the B.S. degree in oceanography from the University of Washington, Seattle, in 1967, the M.S. degree in marine science from the College of Williams and Mary, Williamsburg, VA, in 1971, and the Ph.D. degree in oceanography from the Oregon State University, Corvallis, in 1976.

He began working at the U.S. Naval Ocean Research and Development Activity, now part of the Naval Research Laboratory (NRL), Stennis Space Center, MS, in 1977. Except for a five-year assignment as a Principle Scientist at NATO's SACLANTCEN, La Spezia, Italy (1985–1989), he has worked at NRL as a Research Scientist and is currently the Head of the Seafloor Sciences Branch in the Marine Geosciences Division. His research interests include the effects of biological and physical processes on sediment structure, behavior, and physical properties near the sediment-water interface. His current research is linked to high-frequency acoustic scattering from and propagation within the seafloor and prediction of mine burial.

Dr. Richardson is a Fellow in the Acoustical Society of America, and a member of the American Geophysical Union (AGU), the European Geophysical Society, and Sigma Xi.

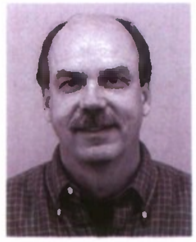

Kevin B. Briggs received the B.S. degree in biology from the Florida Atlantic University, Boca Raton, in 1975, the M.S. degree in zoology from the University of Georgia, Athens, in 1978, and the Ph.D. degree in marine geology and geophysics from the Rosenstiel School of Marine and Atmospheric Science, the University of Miami, Miami, FL, in 1994.

He began working at the U.S. Naval Ocean Research and Development Activity, now part of the U.S. Naval Research Laboratory (NRL), Stennis Space Center, MS, in 1979, where he was involved in research on the effects of environmental processes on sediment geoacoustic properties. He has participated in many shallow-water high-frequency acoustics experiments as an Investigator of geoacoustic and roughness properties of the seafloor. He is currently engaged in research on characterization of sediment interface roughness and volume heterogeneity for high-frequency acoustic modeling. He has over 30 published articles on physical and acoustic properties of the seafloor.

Dr. Briggs is a member of the Acoustical Society of America, the American Geophysical Union, and Sigma Xi.

Paul A. Elmore received the B.S. degree in physics from Millsaps College, Jackson, MS, in 1990 and the Ph.D. degree in physics from the University of Mississippi, Oxford, MS, in 1996 where he was a Graduate Fellow at the National Center for Physical Acoustics.

He received a fellowship from the American Society of Engineering Education to pursue postdoctoral research in ocean acoustics in the Acoustics Division of the U.S. Naval Research Laboratory, Stennis Space Center, MS, from 1996 to 1998. Then, he worked for the U.S. Navy as a Physicist at the U.S. Naval Oceanographic Office from 1998 to 2001, and since 2001, he has been a Research Physicist for the Marine Geosciences Division of the U.S. Naval Research Laboratory. His research interests are in nonlinear acoustics, ocean acoustics, seafloor sensing, and nearshore environmental prediction.

Dr. Elmore is a member of the American Geophysical Union.

Edward F. Braithwaite III received the B.S. degree in information systems and decision science from the A&M College, Louisiana State University, Baton Rouge, in 1999, the M.A. degree in Christian education from the New Orleans Baptist Theological Seminary, New Orleans, LA, in 2002, and the M.S. degree in computer science from the University of Southern Mississippi, Hattiesburg, in 2006.

He began working at the U.S. Naval Research Laboratory, Stennis Space Center, MS, in 2001 as a Computer Support and then as a Computer Scientist supporting programming and data processing of mine burial and other research projects in the Seafloor Sciences branch.

John Bradley received the B.S. and M.S. degrees in electrical engineering from the University of New Orleans, New Orleans, LA, in 1995 and 1997, respectively.

He has been working as a Design Engineer at Omni Technologies, Inc., New Orleans, LA, since 1997 and is involved in the hardware and software development of oceanographic instrumentation and sensors.

Sean Griffin received the B.S. degree in electrical engineering from the Louisiana State University, Shreveport, in 1987 and performed graduate studies at the University of New Orleans, New Orleans, LA.

He cofounded Omni Technologies, Inc., New Orleans, LA, in 1994. He has spent the last 15 years working on oceanographic instrumentation developing a wide array of acoustic, geoacoustic, geotechnica, and specialized sensors and systems for oceanographic purposes.

Thomas F. Wever received the Diploma degree in geophysics and the Ph.D. degree in field of continental crustal studies using reflection seismic methods, both from the Christian-Albrechts-Universität, Kiel, Germany, in 1985 and 1988, respectively.

He spent two months with PRAKLA-SEISMOS (now part of Schlumberger), Hannover, Germany, during his studies at the university and three semesters at Ludwig-Maximilians-Universität, Munich, Germany. Since 1990, he has been a Research Scientists at the Forschungsanstalt der Bundeswehr für Wasserschall und Geophysik (FWG), Kiel, Germany. He started in the field of sonar range prediction and, since 1992, has been working in the field of mine burial prediction and seafloor studies.

Dr. Wever is a member of the American Geophysical Union (AGU) and the European Association of Geoscientists and Engineers (EAGE).

Ralf Lühder received the Diploma degree in electronic engineering from the University of Applied Sciences, Kiel, Germany, in 1992.

He worked for the Fraunhofer Research Group until the end of 1992. Since 1993, he has been with the Forschungsanstalt der Bundeswehr für Wasserschall und Geophysik (FWG), Kiel, Germany, where he works in the geophysics technical support group.